Realization of a Strongly Interacting Fermi Gas of Dipolar Atoms

S. Baier,[1] D. Petter,[1] J. H. Becher,[1,*] A. Patscheider,[1,2] G. Natale,[1] L. Chomaz,[1] M. J. Mark,[1,2] and F. Ferlaino[1,2,†]
[1]*Institut für Experimentalphysik, Universität Innsbruck, Technikerstraße 25, 6020 Innsbruck, Austria*
[2]*Institut für Quantenoptik und Quanteninformation, Österreichische Akademie der Wissenschaften, 6020 Innsbruck, Austria*

(Received 30 March 2018; published 29 August 2018)

We realize a two-component dipolar Fermi gas with tunable interactions, using erbium atoms. Employing a lattice-protection technique, we selectively prepare deeply degenerate mixtures of the two lowest spin states and perform high-resolution Feshbach spectroscopy in an optical dipole trap. We identify a comparatively broad Feshbach resonance and map the interspin scattering length in its vicinity. The Fermi mixture shows a remarkable collisional stability in the strongly interacting regime, providing a first step towards studies of superfluid pairing, crossing from Cooper pairs to bound molecules, in presence of dipole-dipole interactions.

DOI: 10.1103/PhysRevLett.121.093602

The ability to prepare dipolar quantum gases of magnetic atoms [1–6] has enabled fascinating, yet unexpected, observations, emerging from the long-range and anisotropic character of the dipole-dipole interaction (DDI) among particles. In bosonic systems with dominant DDI, this includes d-wave-patterned collapse [7], droplet stabilization [8–10], and roton quasiparticles [11]. With fermions, many-body dipolar phenomena have been investigated only in spin-polarized systems. Here, the DDI competes with the Pauli pressure, rendering dipolar effects much more subtle, as, e.g., their influence on the shape of the Fermi surface [12].

Magnetic atoms further realize high-spin systems; e.g., fermionic Er has 20 available spin states in the lowest hyperfine manifold. In particular, bosonic dipolar spinor gases have been investigated in remarkable experiments with magnetic Cr atoms [13–16], whereas the fermionic counterpart remains rather unexplored in the quantum regime. Scattering experiments with fermionic Dy mixtures slightly above quantum degeneracy showed a large collisional stability against inelastic dipolar relaxation [17], enabling, e.g., the production of long-lived spin-orbit-coupled gases via Raman excitations [18].

As yet, the realization of a two-component dipolar Fermi mixture with tunable interactions has remained elusive. Such a system can disclose fascinating phenomena, from anisotropic quantum phases of matter, e.g., anisotropic Fermi liquids and superfluid pairing [19,20], to dipolar magnetism [21], but also extended Fermi-Hubbard models with off-site interactions [22]. Fermionic Er and Dy are very promising candidates for such studies, given their large magnetic moment. However, the large density of Feshbach resonances (FRs) even in spin-polarized gases [23–25] raises the question of whether stable fermionic quantum mixtures with tunable interactions can be realized with lanthanides.

We here report on a powerful platform to produce a two-component dipolar Fermi gas of pseudospin 1/2 and demonstrate tunability of the interspin interactions. By using highly magnetic ^{167}Er atoms and a three-dimensional (3D) optical lattice as a tool for spin preparation, we perform high-resolution Feshbach spectroscopy and unambiguously identify the spin nature of the different FRs. Among the resonances, we find a well-isolated and comparatively broad interspin FR and precisely measure the interspin scattering length. Our Fermi mixture reveals a remarkable collisional stability in the strongly interacting regime.

Achieving a deterministic preparation of a spin-1/2 mixture and a precise control over the interspin interactions in highly magnetic lanthanide atoms challenges experimental schemes. Indeed, the enormous density of FRs can cause collisional losses and severe heating, limiting the production and preparation of deeply degenerate mixtures at arbitrary magnetic fields (B), where hundreds of FRs might need to be crossed (see, e.g., [18]). Moreover, state-selective preparation of a spin-1/2 system typically requires large B values for which the quadratic Zeeman effect lifts the degeneracy on the Zeeman splitting among consecutive sublevels [17,26].

For these reasons, we establish a technique for collisional protection during the spin preparation (see Fig. 1). In a nutshell, the key production steps are as follows. We produce a spin-polarized degenerate Fermi gas (DFG) in an optical dipole trap (ODT) at low B [1 in Fig. 1(a)] and load the atoms into the lowest band of a deep 3D optical lattice, which acts as a collisional shield [2 in Fig. 1(a)] [27,28]. We then sweep to high B for spin preparation and perform radio-frequency (rf) transfer [3 in Fig. 1(a)], sweep to the desired B, and eventually melt the lattice [4 in Fig. 1(a)].

Experimentally, we prepare a spin-polarized DFG of ^{167}Er atoms in a crossed-beam ODT [5,29] [1 in Fig. 1(a)]. All fermions occupy the lowest Zeeman state $|\downarrow\rangle \equiv |F = 19/2, m_F = -19/2\rangle$ of the ground-state manifold. Here,

 © 2018 American Physical Society

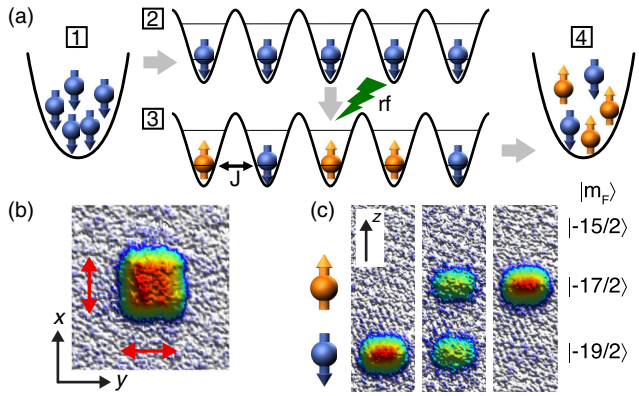

FIG. 1. Spin-1/2 dipolar fermions in a 3D optical lattice. (a) Sketch of the four key stages of our preparation scheme; see text. (b) Band population in the horizontal xy plane, obtained by averaging 50 absorption images for a 12 ms time of flight (TOF). The red arrows indicate the first Brillouin zone of the lattice. (c) Spin-resolved band-mapping images after 9 ms of TOF in the vertical $z\tilde{x}$ plane, where $\tilde{x}$ accounts for the angle between the imaging beam and the y axis of the lattice, for population imbalances $\delta = 1$ (left), 0.02 (middle), and -0.94 (right). The images are averages of about 20 absorption pictures. The spin states are separated along the z direction by a Stern-Gerlach technique.

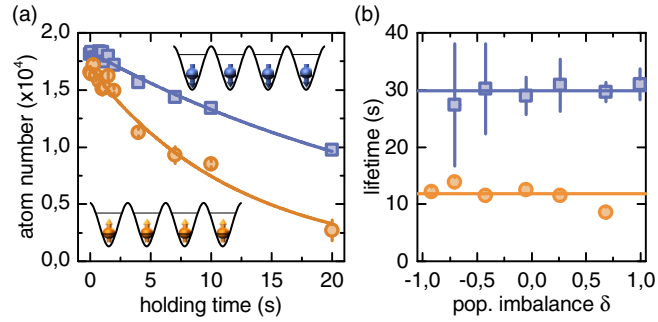

FIG. 2. Spin mixture of dipolar ^{167}Er in a 3D lattice. (a) Lifetime measurements for spin-polarized samples of $|\downarrow\rangle$ (squares) with $\delta = 1$ and of $|\uparrow\rangle$ (circles) with $\delta = -0.92$ at $B = 3.99$ G and their respective exponential decay (solid lines). (b) Lifetimes as a function of δ. Constant fits extract mean lifetimes across δ of $\bar{\tau}_\downarrow = 29.9(3)$ s and $\bar{\tau}_\uparrow = 11.8(7)$ s. All error bars indicate the statistical uncertainty.

F is the total spin quantum number and m_F its projection along the quantization axis. A homogeneous magnetic field of $B = 0.6$ G is applied along the vertical z direction to define the quantization axis and to maintain spin polarization. The sample typically contains $N = 2.4 \times 10^4$ atoms at about $T = 0.25 T_F$. Note that the ODT is shaped to optimize single-band loading of the optical lattice and yields $E_F = k_B \times T_F = k_B \times 170$ nK $= h \times 3.6$ kHz (see Supplemental Material [29]). Here, T_F is the Fermi temperature, h is the Planck constant, and k_B is the Boltzmann constant.

In the next step, we transfer the spin-polarized DFG into a 3D optical lattice [2 in Fig. 1(a)]. Our lattice has a cuboid geometry with lattice spacings $(d_x, d_y, d_z) = (266, 266, 532)$ nm along the three orthogonal directions [29,37]. In order to pin the atoms in a one-fermion-per-lattice-site configuration (unit filling), we use large lattice depths of about $(s_x, s_y, s_z) = (20, 20, 80)$, where s_i with $i \in \{x, y, z\}$ is given in units of the respective recoil energies, $E_{R;x,y} = h \times 4.2$ kHz and $E_{R;z} = h \times 1.05$ kHz. After lattice loading, we obtain a single-component fermionic band insulator (BI) of about 2.2×10^4 $|\downarrow\rangle$ atoms. By melting the lattice and reloading the fermions into the ODT, we measure $T \lesssim 0.3 T_F$ with $N = 2.1 \times 10^4$ ($T_F \approx 160$ nK) and extract a heating rate in the lattice as low as $\dot{T} = 0.03\ T_F/\mathrm{s}$.

Our system is well described by a single-band extended Fermi-Hubbard model [22] with residual tunneling rates of $J_{x,y} = h \times 10.5$ Hz and $J_z = h \times 0.001$ Hz and nearest-neighbor interactions on the order of $h \times 50$ Hz [37]. We confirm the single-band population by performing standard band-mapping measurements [38]. In the horizontal (xy) plane, we do not resolve higher-band occupation [see Fig. 1(b) and Supplemental Material [29]). Along the z axis, we detect a residual $< 5\%$ population in the first excited band, resulting from the fact that $E_F > E_{R,z}$ [39]. Because of the Pauli exclusion principle, doubly occupied sites (doublons) in a single band are strictly forbidden for identical particles ($|\downarrow\rangle$).

In the BI regime, the lattice is expected to provide a strong collisional protection to the particles. As a first application, we use the lattice-protection technique to realize a spinor Fermi gas with pseudospin 1/2 ($|\downarrow\rangle$–$|\uparrow\rangle$), with $|\uparrow\rangle \equiv |F = 19/2, m_F = -17/2\rangle$ [3 in Fig. 1(a)]. Experimentally, we start with a $|\downarrow\rangle$ BI at $B = 0.6$ G and then ramp B in 40 ms to a value of about 40 G, for which the quadratic Zeeman effect in ^{167}Er is large enough to lift the degenerate coupling of the individual spin levels [29]. After letting the field stabilize for 120 ms, we use a standard rf-sweep technique to transfer part of the atoms into the $|\uparrow\rangle$ state. By tuning the rf power, we can precisely control the population imbalance, $\delta = (N_\downarrow - N_\uparrow)/N$, in the mixture, with $N_\downarrow$ ($N_\uparrow$) the number of atoms in $|\downarrow\rangle$ ($|\uparrow\rangle$). Figure 1(c) shows exemplary spin-resolved absorption images of $|\downarrow\rangle$–$|\uparrow\rangle$ mixtures for various δ after B is swept back to low values. We typically record $N = N_\downarrow + N_\uparrow = 1.8 \times 10^4$ and $T \approx 50$ nK after melting the lattice down [4 in Fig. 1(a)]. For comparison, similar measurements in absence of the lattice clearly show a much lower atom number of $N = 0.6 \times 10^4$, proving the strength of our lattice-protection scheme to circumvent losses when cruising through the ultradense Feshbach spectrum [18,23].

Figure 2 shows the high collisional stability of the lattice-confined spin mixture. In particular, we probe $N_{\downarrow,\uparrow}$ as a function of the holding time in the lattice [see Fig. 2(a)]. From an exponential fit to the data, we extract long lifetimes of $\tau_\downarrow = 31(3)$ s and $\tau_\uparrow = 12.2(7)$ s. The measurements are carried out at $B = 3.99$ G, where no FRs

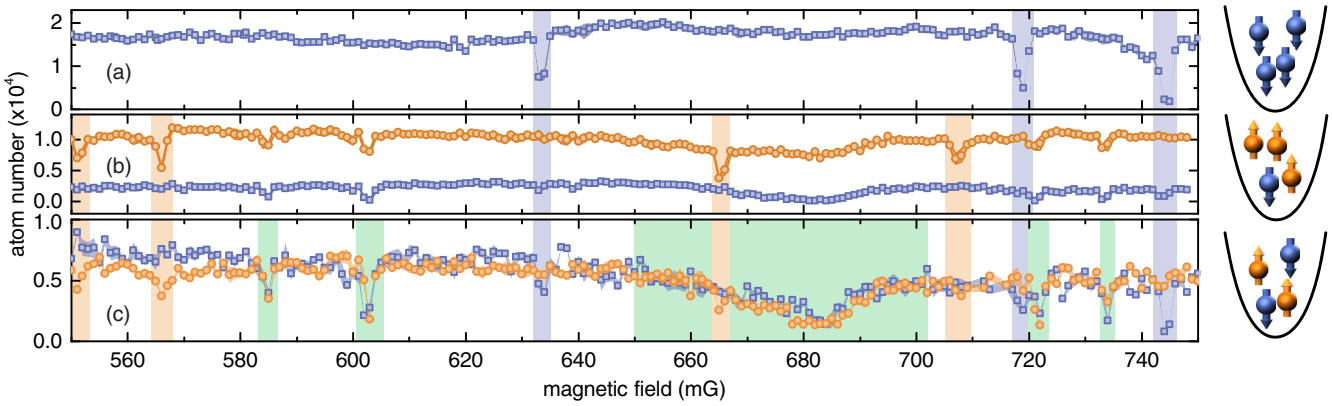

FIG. 3. High-resolution Feshbach spectroscopy for three different population imbalances in an ODT (illustrations): atoms in $|\downarrow\rangle$ (squares) and $|\uparrow\rangle$ (circles) for $\delta = 1$ (a), -0.6 (b), and 0 (c) as a function of B. The determined width and spin nature of the FRs are indicated by the blue ($|\downarrow\rangle$), orange ($|\uparrow\rangle$), and green ($|\downarrow\rangle$–$|\uparrow\rangle$) shaded regions. Each data point is the mean of 2–4 repetitions.

occur (see Supplemental Material [29]). Interestingly, within our error bars, we find no dependence of the lifetime of each spin state on the population in the other state; they remain long regardless of δ [see Fig. 2(b)].

We note that, although very long for our purpose, we always record shorter lifetimes for a $|\uparrow\rangle$ BI with respect to the ones measured for a $|\downarrow\rangle$ BI. Differently from the $|\downarrow\rangle$ case, two-body relaxation processes for $|\uparrow\rangle$ are allowed. At our magnetic fields, this process converts Zeeman energy into a large enough kinetic energy to let the atoms escape from the lattice [13,40] and requires the particles to collide at short distance (on site) [17,41]. In the spin-polarized cases (e.g., $\delta = -1$; $|\uparrow\rangle$), double occupancy necessarily involves population in higher bands since the Pauli exclusion principle forbids doublons in the lowest band. In our system, a continuous transfer of a small fraction of atoms into higher bands might be driven by intensity and frequency noise of the lattice beams [28]. In the case of $|\uparrow\rangle$, this would lead to subsequent fast relaxation and justify the observed difference in the lifetimes.

With our spin-preparation method, we are now able to conduct high-precision Feshbach spectroscopy in an ODT [4 in Fig. 1(a)] in search of interspin loss features. For this, we first prepare the spin-1/2 mixture in a deep lattice at the desired B value. We then transfer the mixture back into the ODT, hold the atoms for 500 ms, and finally measure the spin populations. Figure 3 exemplifies the high-precision Feshbach spectroscopy for three values of δ within a narrow magnetic field range from $B = 550$ to 750 mG with a resolution of 1 mG. A lower-resolution and larger-range scan is shown in the Supplemental Material [29].

As expected [23,24], the atom-number trace as a function of B shows a high density of resonant loss features on top of a constant background. By controlling δ, we are able to distinguish the spin nature of each of the observed FRs. In the excerpt shown in Fig. 3, we identify three narrow homospin FRs in a pure $|\downarrow\rangle$ sample [Fig. 3(a)] and four in a quasipure $|\uparrow\rangle$ sample [Fig. 3(b)]. In the spin-polarized cases, all FRs exhibit widths of the order of our magnetic field stability of $\approx$1 mG. Thanks to our lattice-preparation technique, the shape and the width of the FRs are not affected by the magnetic field ramps, namely, we do not observe neither broadening nor fictitious asymmetry in the loss peaks. For the 50%–50% spin mixture ($\delta = 0$), we observe five additional interspin FRs [Fig. 3(c)], where atoms in the two spin states are simultaneously lost. Because of the complicated scattering behavior of Er, standard coupled-channel methods to assign the leading partial-wave character of the FRs are currently not available [42]. However, the width of the FRs can give indications on the strength of the coupling between open and closed channels [43].

Among the observed interspin FRs, the one at about 0.68 G stands out from the forest of narrow FRs. This FR is almost 2 orders of magnitude broader, making it a promising candidate for Fermi-gas experiments in the strongly interacting regime. We further investigate this FR by performing modulation spectroscopy on the lattice-confined spin-1/2 mixture [3 in Fig. 1(a)] to extract the interspin on-site interaction energy, $U_{\downarrow\uparrow} = U_c + U_{\mathrm{dd}}$, given by the sum of the interspin contact interaction U_c and the DDI U_{dd} [37]. Thanks to the precise knowledge of U_{dd} and to its angle dependence, we are able to directly extract the interspin scattering length, $a_{\downarrow\uparrow} \propto U_c = U_{\downarrow\uparrow} - U_{\mathrm{dd}}$, both in amplitude and in sign (for details, see Supplemental Material [29]).

Figure 4(a) summarizes our results, showing the tunability of $a_{\downarrow\uparrow}$ from positive to negative values across the interspin FR. As a first estimate of the B-to-$a_{\downarrow\uparrow}$ conversion, we use the simple single-channel formula, leading to $a_{\downarrow\uparrow}(B) = a_{\mathrm{bg}}(1 - \Delta/(B - B_0) - \Delta'/(B - B_0'))$ [43]. From the fit to the data, we extract the background scattering length $a_{\mathrm{bg}} = 91(8)a_0$, the position of the comparatively broad FR $B_0 = 687(1)$ mG, and its width $\Delta = 58(6)$ mG. Note that our fitting function also accounts for a nearby interspin FR at $B_0' = 480$ mG (out of range of Figs. 3 and 4) of width $\Delta' = 29(4)$ mG, whereas narrower interspin FRs are neglected. Based on the extracted values, we can estimate an

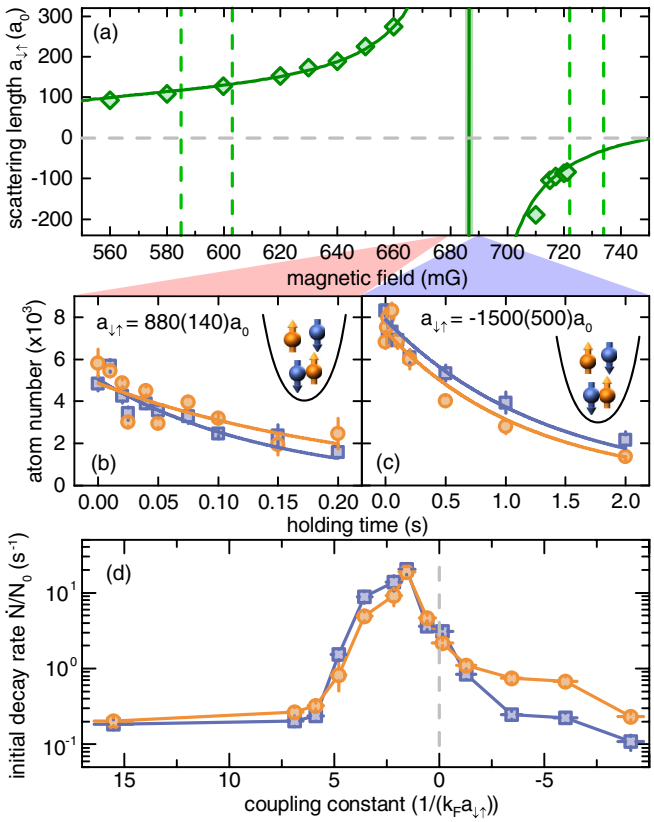

FIG. 4. Interspin scattering length and collisional behavior of the strongly interacting Fermi mixture (a) $a_{\downarrow\uparrow}$ extracted from modulation spectroscopy in the lattice. Error bars are smaller than the size of the data points. Vertical dashed lines indicate the position of narrow interspin FRs as identified in Fig. 3(c). The solid line is a fit to the data with the fit statistical uncertainty indicated as shaded region. (b),(c) Lifetimes of a spin mixture of $|\downarrow\rangle$ (squares) and $|\uparrow\rangle$ (circles) with $\delta = 0$ in an ODT for large positive $a_{\downarrow\uparrow}$ at 680 mG (b) and for large negative $a_{\downarrow\uparrow}$ at 690 mG. (d) Initial decay rate $\dot{N}/N_0$ of the normalized atom numbers as a function of $1/(k_F a_{\downarrow\uparrow})$ in the vicinity of the FR. Error bars on the coupling constant are deduced via standard error propagation.

order of magnitude for the effective range of the FR, $R^* = \hbar^2/(m_{\mathrm{Er}}\Delta a_{\mathrm{bg}}\delta\mu)$ [43]. Here, m_{Er} is the mass of ^{167}Er. The differential magnetic moment between the open and closed channel $\delta\mu$ is not known for the considered FR. However, taking $\delta\mu = 3\mu_B$, which is the typical value measured on bosonic Er_2 [42], we estimate R^* on the order of $1000a_0$. With this order of magnitude, our typical two-component Fermi gases verify $1/k_F R^* \gtrsim 1$, with k_F being the Fermi wave vector [29]. This identifies the intermediate strength of the FR [44], for which the gas is expected to remain strongly interacting at unitarity [45,46].

For strongly interacting alkali Fermi gases, the large collisional stability in two-component mixtures has been essential for observing the crossover from a superfluid of delocalized pairs along the Bardeen-Cooper-Schrieffer (BCS) mechanism to a Bose-Einstein condensate (BEC) of bound molecules [47]. As a direct consequence of the Pauli principle, three-body recombination occurs primarily on the repulsive (BEC) side of broad s-wave FRs, where a weakly bound molecular level exists [48], whereas on the attractive (BCS) side, large scattering lengths coexist with a remarkable collisional stability [49–52]. Such an asymmetry in the scattering behavior is identified as an essential attribute of BEC-BCS physics.

We investigate this aspect in a second set of experiments. We prepare an equally populated spin mixture ($\delta = 0$) in an ODT [4 in Fig. 1(a)] and probe the time evolution of the spin population as a function of the holding time in the trap for various B across the FR. Exemplary decay curves are shown in Figs. 4(b) and 4(c). On the BEC side, at $a_{\downarrow\uparrow} = 880(140)\ a_0$, we observe a fast decay of both $|\uparrow\rangle$ and $|\downarrow\rangle$ atoms [Fig. 4(b)]. A simple exponential fit to the data gives lifetimes of $\tau_{1/e} \approx 150$ ms. In contrast, on the BCS side at $a_{\downarrow\uparrow} = -1500(500)\ a_0$ [Fig. 4(d)], the spin mixture shows a large collisional stability with lifetimes exceeding $\tau_{1/e} = 1200$ ms [Fig. 4(c)].

To get deeper insights, we systematically study the initial decay rate $\dot{N}/N_0$ as a function of B. We determine the rates by using a linear fit to the data for the initial time evolution. Figure 4(d) summarizes our results, plotted in terms of the dimensionless coupling constant $1/(k_F a_{\downarrow\uparrow})$. We observe an asymmetry of the loss rate curve, indicating that the Fermi mixture is remarkably stable in the unitary and strongly attractive regime. We note that both the qualitative shape and the quantitative values of the loss rates in ^{167}Er show strong similarities to the ones measured in ^{40}K [51].

The existence of a comparatively broad interspin FR and our demonstration of the interaction tuning across this resonance make fermionic Er gases a promising system for accessing BEC-BCS crossover physics within a distinct scattering scenario. Indeed, our mixture adds both the DDI and an intermediate effective range in the short-range scattering compared to the alkali cases [46,47], paving the way for studying exotic Cooper pairs and molecular BECs [19,44,53] and calling for new theory developments [54].

We thank R. Grimm, M. Greiner, and A. M. Rey for fruitful discussions. We acknowledge financial support through an ERC Consolidator Grant (RARE, No. 681432), FET Proactive Project (RySQ, No. 640378) of the EU H2020, and a DFG/FWF (FOR 2247). L. C. is supported within a Marie Curie Project (DipPhase, No. 706809) of the EU H2020.

*Present address: Physikalisches Institut, Universität Heidelberg, Im Neuenheimer Feld 226, 69120 Heidelberg, Germany.

†To whom all correspondence should be addressed. francesca.ferlaino@uibk.ac.at

[1] A. Griesmaier, J. Werner, S. Hensler, J. Stuhler, and T. Pfau, Phys. Rev. Lett. **94**, 160401 (2005).
[2] M. Lu, N. Q. Burdick, S. H. Youn, and B. L. Lev, Phys. Rev. Lett. **107**, 190401 (2011).
[3] M. Lu, N. Q. Burdick, and B. L. Lev, Phys. Rev. Lett. **108**, 215301 (2012).
[4] K. Aikawa, A. Frisch, M. Mark, S. Baier, A. Rietzler, R. Grimm, and F. Ferlaino, Phys. Rev. Lett. **108**, 210401 (2012).
[5] K. Aikawa, A. Frisch, M. Mark, S. Baier, R. Grimm, and F. Ferlaino, Phys. Rev. Lett. **112**, 010404 (2014).
[6] B. Naylor, A. Reigue, E. Maréchal, O. Gorceix, B. Laburthe-Tolra, and L. Vernac, Phys. Rev. A **91**, 011603 (2015).
[7] T. Lahaye, J. Metz, B. Fröhlich, T. Koch, M. Meister, A. Griesmaier, T. Pfau, H. Saito, Y. Kawaguchi, and M. Ueda, Phys. Rev. Lett. **101**, 080401 (2008).
[8] H. Kadau, M. Schmitt, M. Wenzel, C. Wink, T. Maier, I. Ferrier-Barbut, and P. Tilman, Nature (London) **530**, 194 (2016).
[9] L. Chomaz, S. Baier, D. Petter, M. J. Mark, F. Wächtler, L. Santos, and F. Ferlaino, Phys. Rev. X **6**, 041039 (2016).
[10] M. Schmitt, M. Wenzel, F. Böttcher, I. Ferrier-Barbut, and T. Pfau, Nature (London) **539**, 259 (2016).
[11] L. Chomaz, R. M. W. van Bijnen, D. Petter, G. Faraoni, S. Baier, J. H. Becher, M. J. Mark, F. Waechtler, L. Santos, and F. Ferlaino, Nat. Phys. **14**, 442 (2018).
[12] K. Aikawa, S. Baier, A. Frisch, M. Mark, C. Ravensbergen, and F. Ferlaino, Science **345**, 1484 (2014).
[13] S. Hensler, J. Werner, A. Griesmaier, P. Schmidt, A. Görlitz, T. Pfau, S. Giovanazzi, and K. Rzażewski, Appl. Phys. B **77**, 765 (2003).
[14] B. Pasquiou, E. Maréchal, G. Bismut, P. Pedri, L. Vernac, O. Gorceix, and B. Laburthe-Tolra, Phys. Rev. Lett. **106**, 255303 (2011).
[15] A. de Paz, A. Sharma, A. Chotia, E. Maréchal, J. H. Huckans, P. Pedri, L. Santos, O. Gorceix, L. Vernac, and B. Laburthe-Tolra, Phys. Rev. Lett. **111**, 185305 (2013).
[16] S. Lepoutre, J. Schachenmayer, L. Gabardos, B. Zhu, B. Naylor, E. Marechal, O. Gorceix, A. M. Rey, L. Vernac, and B. Laburthe-Tolra, arXiv:1803.02628.
[17] N. Q. Burdick, K. Baumann, Y. Tang, M. Lu, and B. L. Lev, Phys. Rev. Lett. **114**, 023201 (2015).
[18] N. Q. Burdick, Y. Tang, and B. L. Lev, Phys. Rev. X **6**, 031022 (2016).
[19] M. A. Baranov, M. Dalmonte, G. Pupillo, and P. Zoller, Chem. Rev. **112**, 5012 (2012).
[20] I. Bloch, J. Dalibard, and W. Zwerger, Rev. Mod. Phys. **80**, 885 (2008).
[21] D. M. Stamper-Kurn and M. Ueda, Rev. Mod. Phys. **85**, 1191 (2013).
[22] O. Dutta, M. Gajda, P. Hauke, M. Lewenstein, D.-S. Lühmann, B. A. Malomed, T. Sowiński, and J. Zakrzewski, Rep. Prog. Phys. **78**, 066001 (2015).
[23] A. Frisch, M. Mark, K. Aikawa, F. Ferlaino, J. Bohn, C. Makrides, A. Petrov, and S. Kotochigova, Nature (London) **507**, 475 (2014).
[24] K. Baumann, N. Q. Burdick, M. Lu, and B. L. Lev, Phys. Rev. A **89**, 020701 (2014).
[25] T. Maier, H. Kadau, M. Schmitt, M. Wenzel, I. Ferrier-Barbut, T. Pfau, A. Frisch, S. Baier, K. Aikawa, L. Chomaz, M. J. Mark, F. Ferlaino, C. Makrides, E. Tiesinga, A. Petrov, and S. Kotochigova, Phys. Rev. X **5**, 041029 (2015).
[26] H. Schmaljohann, M. Erhard, J. Kronjäger, M. Kottke, S. van Staa, L. Cacciapuoti, J. J. Arlt, K. Bongs, and K. Sengstock, Phys. Rev. Lett. **92**, 040402 (2004).
[27] K. Winkler, F. Lang, G. Thalhammer, P. v. d. Straten, R. Grimm, and J. H. Denschlag, Phys. Rev. Lett. **98**, 043201 (2007).
[28] A. Chotia, B. Neyenhuis, S. A. Moses, B. Yan, J. P. Covey, M. Foss-Feig, A. M. Rey, D. S. Jin, and J. Ye, Phys. Rev. Lett. **108**, 080405 (2012).
[29] See Supplemental Material at http://link.aps.org/supplemental/10.1103/PhysRevLett.121.093602, which includes Refs. [30–36], for details on the experimental preparation and measurement schemes.
[30] M. Köhl, H. Moritz, T. Stöferle, K. Günter, and T. Esslinger, Phys. Rev. Lett. **94**, 080403 (2005).
[31] J. G. Conway and B. G. Wybourne, Phys. Rev. **130**, 2325 (1963).
[32] K. F. Smith and P. J. Unsworth, Proc. Phys. Soc. **86**, 1249 (1965).
[33] B. Yan, S. A. Moses, B. Gadway, J. P. Covey, K. R. A. Hazzard, A. M. Rey, D. S. Jin, and J. Ye, Nature (London) **501**, 521 (2013).
[34] S. Baier *et al.* (to be published).
[35] J. H. Becher, S. Baier, K. Aikawa, M. Lepers, J.-F. Wyart, O. Dulieu, and F. Ferlaino, Phys. Rev. A **97**, 012509 (2018).
[36] R. Jördens, N. Strohmaier, K. Günter, H. Moritz, and T. Essslinger, Nature (London) **455**, 204 (2008).
[37] S. Baier, M. J. Mark, D. Petter, K. Aikawa, L. Chomaz, Z. Cai, M. Baranov, P. Zoller, and F. Ferlaino, Science **352**, 201 (2016).
[38] A. Kastberg, W. D. Phillips, S. L. Rolston, R. J. C. Spreeuw, and P. S. Jessen, Phys. Rev. Lett. **74**, 1542 (1995).
[39] S. Will, Ph.D. thesis, Johannes Gutenberg-Universität, Mainz (2011).
[40] A. de Paz, A. Chotia, E. Maréchal, P. Pedri, L. Vernac, O. Gorceix, and B. Laburthe-Tolra, Phys. Rev. A **87**, 051609 (2013).
[41] B. Pasquiou, G. Bismut, Q. Beaufils, A. Crubellier, E. Maréchal, P. Pedri, L. Vernac, O. Gorceix, and B. Laburthe-Tolra, Phys. Rev. A **81**, 042716 (2010).
[42] A. Frisch, M. Mark, K. Aikawa, S. Baier, R. Grimm, A. Petrov, S. Kotochigova, G. Quéméner, M. Lepers, O. Dulieu, and F. Ferlaino, Phys. Rev. Lett. **115**, 203201 (2015).
[43] C. Chin, R. Grimm, P. Julienne, and E. Tiesinga, Rev. Mod. Phys. **82**, 1225 (2010).
[44] V. Gurarie and L. Radzihovsky, Ann. Phys. (Amsterdam), Spec. Issue **322**, 2 (2007).
[45] T.-L. Ho, X. Cui, and W. Li, Phys. Rev. Lett. **108**, 250401 (2012).
[46] E. L. Hazlett, Y. Zhang, R. W. Stites, and K. M. O'Hara, Phys. Rev. Lett. **108**, 045304 (2012).

[47] *Proceedings of the International School of Physics "Enrico Fermi", Course CLXIV*, edited by M. Inguscio, W. Ketterle, and C. Salomon (IOS Press, Amsterdam, 2007).
[48] D. S. Petrov, Phys. Rev. A **67**, 010703 (2003).
[49] K. Dieckmann, C. A. Stan, S. Gupta, Z. Hadzibabic, C. H. Schunck, and W. Ketterle, Phys. Rev. Lett. **89**, 203201 (2002).
[50] T. Bourdel, J. Cubizolles, L. Khaykovich, K. M. F. Magalhães, S. J. J. M. F. Kokkelmans, G. V. Shlyapnikov, and C. Salomon, Phys. Rev. Lett. **91**, 020402 (2003).
[51] C. A. Regal, M. Greiner, and D. S. Jin, Phys. Rev. Lett. **92**, 083201 (2004).
[52] S. Jochim, Ph.D. thesis, Leopold-Franzens-Universität, Innsbruck (2004).
[53] A. Schwenk and C. J. Pethick, Phys. Rev. Lett. **95**, 160401 (2005).
[54] M. Li, E. Tiesinga, and S. Kotochigova, Phys. Rev. A **97**, 053627 (2018).